

ADA029980

BEST AVAILABLE COPY

12  
6.5.

# Effects of Thermal-Mechanical Processing on the Microyield Strength of Invar

Materials Sciences Laboratory  
Laboratory Operations  
The Aerospace Corporation  
El Segundo, Calif. 90245

12 August 1976

Interim Report

D D C  
REF ID: A65414  
DISTRIBUTED  
SEP 15 1976  
C

APPROVED FOR PUBLIC RELEASE;  
DISTRIBUTION UNLIMITED

Prepared for  
SPACE AND MISSILE SYSTEMS ORGANIZATION  
AIR FORCE SYSTEMS COMMAND  
Los Angeles Air Force Station  
P.O. Box 92960, Worldway Postal Center  
Los Angeles, Calif. 90009

BEST AVAILABLE COPY

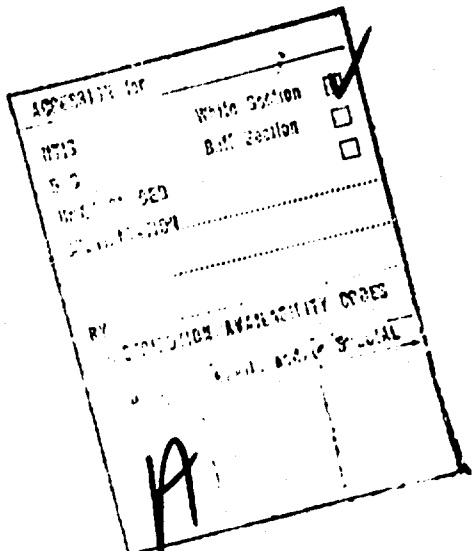
This report was submitted by The Aerospace Corporation, El Segundo, CA 90245, under Contract F04701-75-C-0076 with the Space and Missile Systems Organization, Deputy for Advanced Space Programs, P.O. Box 92960, Worldway Postal Center, Los Angeles, CA 90009. It was reviewed and approved for The Aerospace Corporation by W. C. Riley, Director, Materials Sciences Laboratory. Lt. Ronald C. Lawson, SAMSO/YAPT, was the project officer.

This report has been reviewed by the Information Office (OI) and is releasable to the National Technical Information Service (NTIS). At NTIS, it will be available to the general public, including foreign nations.

This technical report has been reviewed and is approved for publication. Publication of this report does not constitute Air Force approval of the report's findings or conclusions. It is published only for the exchange and stimulation of ideas.

FOR THE COMMANDER

Ronald C. Lawson  
Ronald C. Lawson  
1st Lieutenant, USAF  
Technology Plans Division  
Deputy for Advanced Space Programs



## UNCLASSIFIED

SECURITY CLASSIFICATION OF THIS PAGE (When Data Entered)

11 REPORT DOCUMENTATION PAGE			READ INSTRUCTIONS BEFORE COMPLETING FORM	
1. REPORT NUMBER SAMSO-TR-76-191	2. GOVT ACCESSION NO.	3. RECIPIENT'S CATALOG NUMBER 9) Technical Rep.	4. TYPE OF REPORT & PERIOD COVERED Interim	
6) EFFECTS OF THERMAL-MECHANICAL PROCESSING ON THE MICROYIELD STRENGTH OF INVAR			5. PERFORMING ORG. REPORT NUMBER 14) TR-0076 (6950-07)-5	
7. AUTHORAL 10) E. G. Wolff, C. S. Susskind, D. L. Dull			8. CONTRACT OR GRANT NUMBER 15) F04701-75-C-0076	
9. PERFORMING ORGANIZATION NAME AND ADDRESS The Aerospace Corporation El Segundo, Calif. 90245			10. PROGRAM ELEMENT, PROJECT, TASK AREA & WORK UNIT NUMBERS 12) 36p.	
11. CONTROLLING OFFICE NAME AND ADDRESS Space and Missile Systems Organization Air Force Systems Command Los Angeles, Calif. 90009			11. REPORT DATE 12 Aug 1976	
14. MONITORING AGENCY NAME & ADDRESS (if different from Controlling Office)			12. NUMBER OF PAGES 29	
			15. SECURITY CLASS. (of this report) Unclassified	
			15a. DECLASSIFICATION/DOWNGRADING SCHEDULE	
16. DISTRIBUTION STATEMENT (of this Report) Approved for public release; distribution unlimited				
17. DISTRIBUTION STATEMENT (of the abstract entered in Block 20, if different from Report)				
18. SUPPLEMENTARY NOTES				
19. KEY WORDS (Continue on reverse side if necessary and identify by block number) Microyield Strength Thermal-Mechanical Processing				
20. ABSTRACT (Continue on reverse side if necessary and identify by block number) Microyield strengths (MYS) were determined for 20- and 40-mil Invar sheet, 0.5-in.-diam rod, and 0.5-in.-diam (1/32 wall thickness) tube using resistance strain gages. The various shapes were also characterized in terms of metallography and mechanical properties. Several heat treatments were studied for each shape. The MYS ranged from 9 to 31 ksi (62 to 214 MPa). Stretched sheet had the highest MYS. Slow furnace cooling increased the MYS of rod and tube. Stress versus plastic strain curves were characterized by				

**UNCLASSIFIED**

**SECURITY CLASSIFICATION OF THIS PAGE(When Data Entered)**

**19. KEY WORDS (Continued)**

**20. ABSTRACT (Continued)**

the logarithmic relationship  $\sigma \propto K \epsilon_p^n$ . Two sets of K and n (below and above the MYS) were determined for sheet with 2% stretching.

$$* \sigma = K \epsilon_p^n$$

**UNCLASSIFIED**

**SECURITY CLASSIFICATION OF THIS PAGE(When Data Entered)**

## PREFACE

This report is the first of a series describing the results from a research program on the dimensional stability of Invar. Subsequent reports will summarize the results of dimensional changes under zero stress conditions, microcreep, and the thermal expansion coefficient in the temperature range 25 to 150°C.

Contributors to the research program since its initiation in July 1971 include the following:

T. J. Bertone	Metallography
D. L. Dull	Microyield Strength
S. A. Eselun	Thermal Expansion
A. N. Ewing	Thermal Expansion
L. F. Goldstein	Optics Consultant
K. T. Kamber	Technical Consultant
E. G. Kendall	Administrative Support
L. King	Data Reduction
M. Lachuk	Thermal Expansion
B. Larsen	Data Reduction
W. M. Leveroni	Program Office Monitor
L. Raymond	Administrative Support
J. H. Richardson	Laser Interferometry
H. Smallen	Program Administration
J. K. Stanley	Initial Technical Director
C. S. Susskind	Strain Gage Techniques
J. S. Thompson	Thermal Expansion
E. G. Wolff	Technical Director after October 1973.

## CONTENTS

PREFACE .....	1
I. INTRODUCTION .....	5
II. EXPERIMENTAL PROCEDURE .....	9
A. Specimen Preparation .....	9
B. Microyield Strength Testing .....	13
III. RESULTS AND DISCUSSION .....	17
A. Metallography .....	17
B. Mechanical Properties .....	17
C. Microyield Strength .....	21
D. Stress Versus Plastic Strain Curves .....	23
REFERENCES .....	29

## TABLES

1. Chemical Compositions of Invar Shapes .....	10
2. Heat Treatments of Invar .....	12
3. Microyield Strength and Mechanical Properties of Invar Shapes .....	22
4. Results from Statistical Analysis for the Determination of K and n .....	28

## FIGURES

1. Specimen configurations used for Invar program . . . . .	11
2. Experimental test setup for MYS determination . . . . .	14
3. Plot of cumulative plastic microstrain versus cumulative time at stress. (The applied stress was 22.1 ksi, i.e., the MYS.) . . . . .	15
4. Optical micrograph of as-received Invar 20-mil sheet in longitudinal direction . . . . .	18
5. Optical micrograph of Invar 40-mil sheet (40-2 heat treatment) in longitudinal direction . . . . .	18
6. Optical micrograph of Invar rod (R-1 heat treatment) in radial direction . . . . .	19
7. Optical micrograph of Invar tube (T-1 heat treatment) in radial direction . . . . .	19
8. SEM micrograph of Invar 40-mil sheet (40-1 heat treatment) in longitudinal direction showing square areas A and B used for EDAX . . . . .	20
9. EDAX of Invar 40-mil sheet in square areas A and B shown in Fig. 8. (The two highest intensities correspond to Fe and Ni, respectively.) . . . . .	20
10. Stress-plastic strain curve of a 20-mil sheet . . . . .	24
11. Stress-plastic strain curves of 40-mil sheet . . . . .	25
12. Log-log plot of stress-plastic strain curve of 40-mil sheet (40-2-L) . . . . .	27

## I. INTRODUCTION

Dimensional stability is defined as the ability of a material to resist permanent dimensional changes caused by externally applied stresses, temperature excursions, redistribution of residual stresses, or metallurgical phase instability. Dimensional changes in materials caused by externally applied stress are important to the designer of precision instruments. Most materials plastically deform at a stress significantly lower than the conventional 0.2% offset yield strength, i. e., stress required to produce 2000 microstrain ( $\mu\epsilon$ ) of plastic strain. The conventional yield strength is of little use to the designer who must know the stress that produces a plastic strain of 1  $\mu\epsilon$ . For a precise method for measuring the stress to produce such small plastic strains, precision strain-gage techniques are used. This method involves loading and unloading a material to successively higher stresses and measuring the residual plastic strain between each loading step. The microyield strength (MYS) is defined as the stress required to produce a plastic strain of 1  $\mu\epsilon$ .

The purpose of this study was to determine how thermal-mechanical processing could be used to increase the MYS of Invar sheet, rod, and tube. A high MYS is desired to minimize dimensional changes due to microcreep during short-term loading. The thermal-mechanical treatments include austenitizing followed by water quenching, long-time thermal treatment at low and high temperatures followed by air or furnace cooling, and stretching, i. e., cold-working.

In 1896, Giullaume<sup>1</sup> discovered that iron with 36% nickel exhibited an unusually low thermal expansion coefficient. Invar, the name given to this alloy, is used today for optical components, optical component housing, microwave filters, interconnectors for solar cells, cryogenic piping, waveguides, temperature regulators, and TV camera supports for space probes. Compared to low-thermal expansion ceramics or composites, Invar has better machinability, higher thermal and electrical conductivity, higher thermal

shock resistance, better magnetic properties, better vacuum stability, and more moderate cost.<sup>2</sup> The principal disadvantages are the relatively high density and the limited temperature range for a low thermal expansion coefficient and dimensional instability, which are dependent on thermal-mechanical processing and chemical composition.

There have been relatively few investigations reported to date on the MYS of Invar and its alloys. Hordon and Weihrauch<sup>3</sup> studied Invar "36" (0.12% C, 1% Mn, and 0.35% Si) using capacitance strain gages. The Invar was solution-treated at 830°C, quenched, rough-machined, stress-relieved at 650°C, air cooled, finished-machined, and stabilized at 93°C for 48 hr with air cooling. The elastic limit was defined as the stress at which a plastic strain was first detected. Loads were applied in increments of 400 psi at rates of 20 ksi/min with immediate unloading when the stress was reached. They reported the elastic limit to be 26.4 ksi. Extensive MYS studies of Ni-Span-C (42% Ni, 5-6% Cr, 2.5% Ti, 0.5% Al, <0.06% C, and balance Fe) were performed using the strain-gage techniques of Ingram et al.<sup>4</sup> Samples were rough-machined, solution-treated at 980°C for 1-1/4 hr, water-quenched, annealed at 677°C for 21 hr, air-cooled, and finished-machined. Incremental tensile loading at 0.05 in./min cross-head speed with immediate unloading was employed. Strain sensitivity was reported to be  $1 \times 10^{-7}$  in./in. with a scatter of  $\pm 3 \times 10^{-7}$  in./in. The MYS for Ni Span-C averaged 39 ksi. Schetky<sup>5</sup> reported 47 ksi for the MYS of Ni-Span-C. Marschall\* reported that Universal Cyclops LR (low residual impurity content)<sup>6</sup> and Fe-36% Ni (commercial levels of impurities) have a MYS of 6 to 10 ksi. Cold-drawing (35% reduction) increased the MYS to 45 to 49 ksi. Geil and Feinberg<sup>7</sup> also reported that the MYS of annealed Invar was  $\leq 10$  ksi. Geil et al.<sup>8</sup> also showed that the thermal heating resulting from plastic deformation during MYS testing was negligible. Hemmings and Perkins<sup>9</sup> reported

\* C. W. Marschall, Battelle Columbus Laboratories, private communication, 2 July 1975.

that the MYS ranged from 6 to 24 ksi for Fe-36% Ni with <0.1% C. The higher MYS values were obtained by using slower cooling rates in the 200 to 400°C temperature range. Marschall<sup>10</sup> reported that the reduction of the carbon content from 0.077 to 0.01% does not significantly affect the MYS of 1-mm-thick UNISPAN LR 35 sheet. All decarburized specimens had a MYS between 10 and 18 ksi.

## II EXPERIMENTAL PROCEDURE

A. SPECIMEN PREPARATION

The chemical composition of each shape is given in Table I. The chemical composition requirements for Invar in accordance with the LR 35 specification is included. All shapes except the 20-mil sheet met the chemical composition requirements. The silicon content in the 20-mil sheet, i.e., 0.063% Si, slightly exceeded the specified maximum, i.e., 0.05% Si.

The specimen configurations used for MYS and mechanical properties testing of sheet and rod are shown in Fig. 1. The tube specimen (not shown) was approximately 12-in. long with 1/4-in.-diam holes drilled 1 in. from the tube ends. The sheet specimens were machined from 20- and 40-mil thick sheet in the transverse and longitudinal directions in the as-received (AR) condition. Three to six sheet and tube specimens were thermal-processed per treatment (Table II).

The rod specimens were rough-machined from oversize 1/2-in.-diam rod stock to within 0.10 in. of the required dimensions. Three specimens were thermal-processed per treatment (Table II). The following sequential machining procedures were performed to reduce surface residual stresses from thermal processing in the specimens:

1. 0.030 in. max cut to within 0.030 in. of final surface.
2. 0.020 in. max cut to within 0.020 in. of final surface.
3. 0.010 in. max cut to within 0.010 in. of final surface.
4. 0.005 in. max cut to within 0.005 in. of final surface.
5. 0.003 in. max cut to within 0.003 in. of final surface.
6. The final cut not to exceed 0.002 in.

The specimens were chemically milled using an acid solution for the remaining 0.002 in. The acid solution, which was recommended by Muller\*

\*Hugh H. Muller, Alcoa, Carson, California, private communication.

Table I. Chemical Compositions of Invar Shapes

Element	20-mil. Sheet	40-mil Sheet	1/2-in.-diam Rod	1/2-in.-diam Tube	LR 35
Al	-	-	<0.022	-	-
C	0.04	0.062	0.056	0.06	0.10 max
Co	-	-	<0.03	-	-
Cr	<0.0005	0.01	<0.01	-	-
Cu	<0.0005	-	<0.03	-	-
Fe	Balance	Balance	Balance	Balance	Balance
H	-	-	0.0029	-	-
Mg	-	0.0045	-	<0.05	-
Mn	0.023	0.01	<0.02	<0.01	0.05 max
Mo	-	0.01	<0.02	-	-
N	0.010	-	0.001	-	-
Ni	36.4	36.1	36.2	36.2	36.5 max
N <sub>2</sub>	-	0.001	-	25 ppm	-
O <sub>2</sub>	-	0.0015	-	25 ppm	-
P	-	0.006	0.001	-	-
Pb	0.12	-	-	-	-
S	-	0.001	0.007	-	-
Si	0.063	0.01	<0.003	-	0.05 max
Sn	-	-	<0.003	-	-

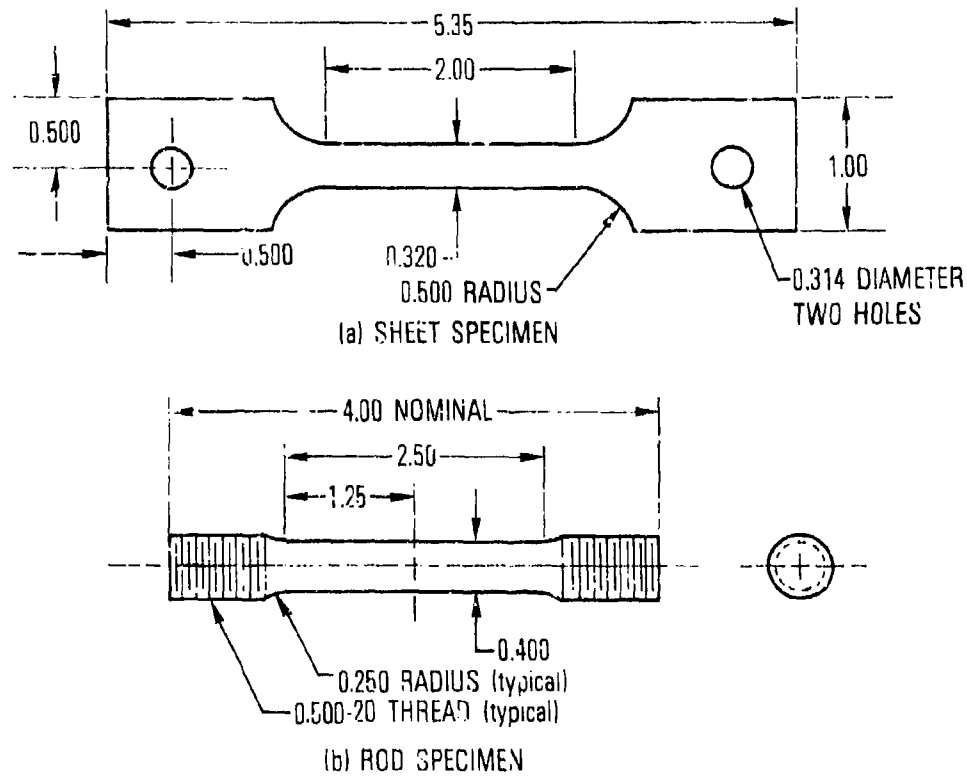


Fig. 1. Specimen configurations used for Invar program

Table II. Heat Treatments of Invar

Material Shape	Identification	Heat Treatment
20-mil Sheet	20- AR	830°C for 20 min, WQ, 430°C salt bath, 1/2% longitudinal stretch
	20-1	AR, 220°C for 24 hr, AC
	20-2	AR, 220°C for 92 hr, AC
40-mil Sheet	40- AR	840°C for 30 min, WQ, 93°C for 4 hr, AC, 2% longitudinal stretch
	40-1	AR, 220°C for 48 hr, FC
	40-2	AR, 320°C for 1 hr, AC, 96°C for 66 hr, AC
1/2-in.-diam Rod	R- AR	Not known
	R-1	AR, 830°C for 30 min, WQ, 315°C for 1 hr, AC, 96°C for 48 hr
	R-2	AR, 830°C for 30 min, WQ, 205°C for 1 hr, AC, 70°C for 48 hr, AC
	R-3	AR, 830°C for 30 min, FC
1/2-in.-diam Tube	T- AR	840°C, WQ, 370°C, salt bath, FC
	T-1	AR, 200°C for 48 hr, FC

WQ = water quench; AR = as-received; AC = air-cool; FC = furnace cool

consisted of: 58 ml  $H_3PO_4$  (75%, 12 N), 11.5 ml HF (70%, 44 N), 106 ml  $HNO_3$  (42° Balme, 15 N) 58 g  $Fe(NO_3)_3 \cdot 6 H_2O$ , and 562 g  $FeCl_3 \cdot 6 H_2O$ .

Linear alkylate sulfuric acid (0.25 g) (wetting agent, Turcoform) was dissolved in distilled water to make 1 liter of solution. The solution was contained in polypropylene beakers. The specimens were immersed in the acid solution for 2 min at 63°C.

#### B. MICROYIELD STRENGTH TESTING

A four strain-gage bridge circuit was used for MYS testing. Two active strain gages were mounted on each MYS specimen located on opposing sides. Two dummy strain gages were mounted on a control specimen for temperature compensation. Micro-Measurements (SA-00-500BH-120) strain gages were cemented on the MYS specimen with Micro-Measurements M-Bond 200 and catalyst.<sup>11</sup> Curing was at room temperature.

A. Vishay/Intertechnology Model V/E-20 high sensitivity digital strain indicator with internal calibration was used to measure strain. An Instron testing machine was used to load the specimen. The crosshead speed was 0.020 in./min during loading and unloading. Testing of the MYS specimens was performed at room temperature in a plexiglass chamber (Fig. 2). The room temperature was constant within  $\pm 0.5^\circ C$  during the test period. Oscillations of the system in the unloaded condition averaged  $\pm 1$  count, which corresponded to a sensitivity of  $\pm 0.1 \mu\epsilon$ .

Initial tests were made on the 20-mil sheet samples. The stability criterion used was based on loading the sample to between 10 to 25% of the anticipated MYS three times using wedge type grips with pins and then unloading. The absolute strain readings fell within  $\pm 0.1 \mu\epsilon$ . The strain gages were considered stable if the strain readout showed no drift with time and varied within  $\pm 1$  count. If stability was not attained, the specimen was regaged.

The specimen was then reloaded to 40% of the anticipated microyield load and held for 1 min and unloaded. A strain indicator reading was taken

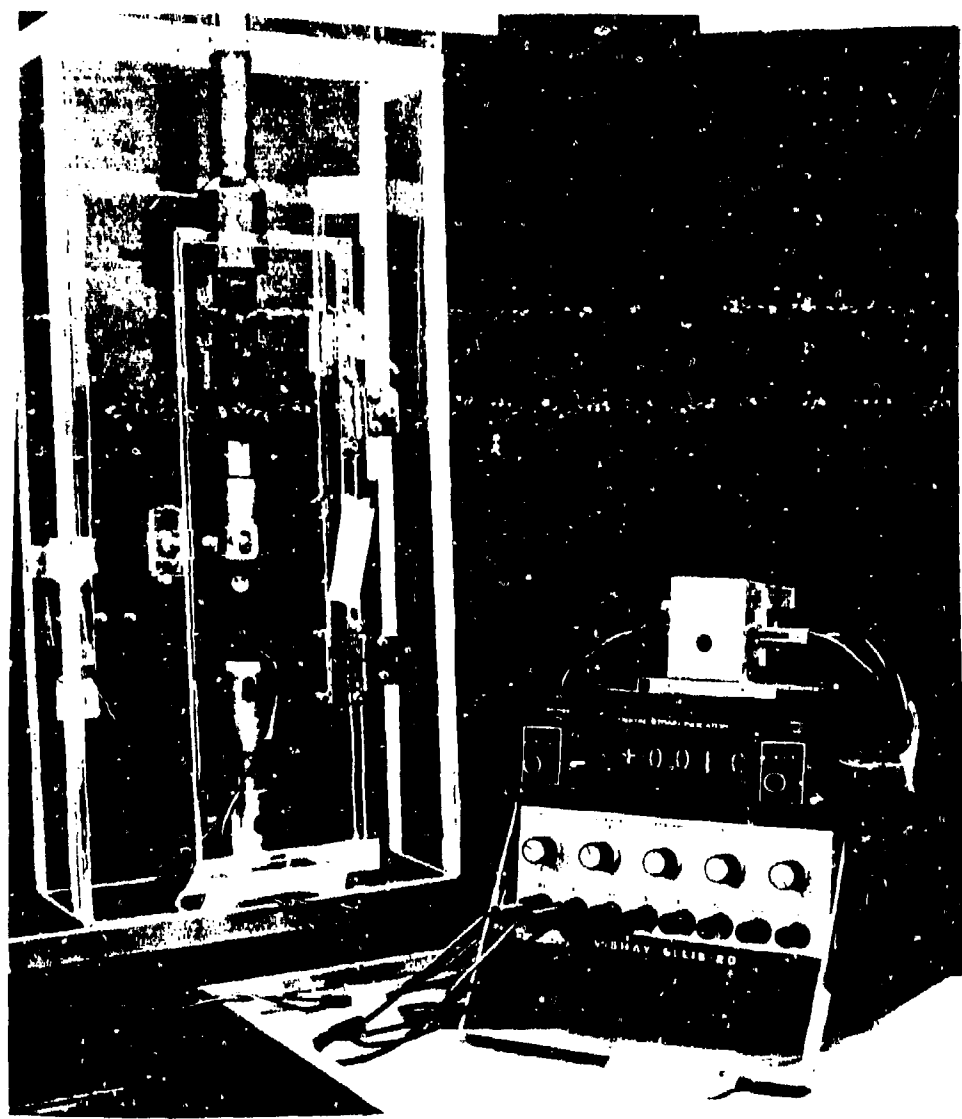


Fig. 2. Experimental test setup for MYS determination

after 3 to 5 min, which was the average time required for the specimen to become stable. Between 4 and 15 successively higher load cycles were employed to reach one unit of plastic microstrain. The test continued until at least 30  $\mu\epsilon$  units of plastic strain were attained.

The effect of time at stress was investigated by successively loading a 20-mil sheet sample to 22.1 ksi (the measured MYS in this case). The microcreep is 0.44  $\mu\epsilon/\text{min}$  (Fig. 3). It was concluded that the 1-min time at stress had no significant effect on MYS determination.

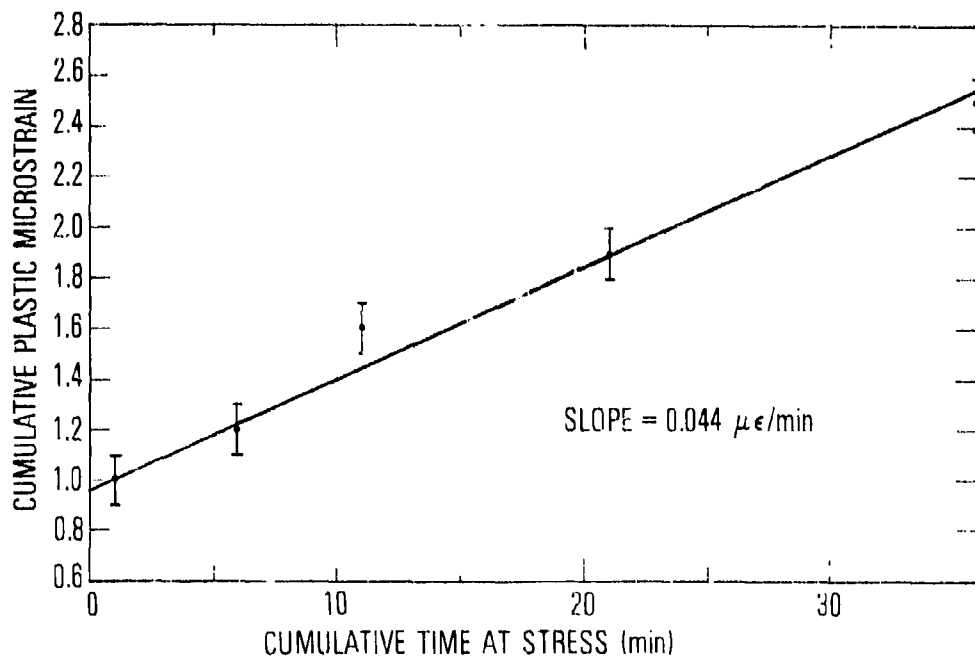


Fig. 3. Plot of cumulative plastic microstrain versus cumulative time at stress. (The applied stress was 22.1 ksi, i.e., the MYS.)

## III. RESULTS AND DISCUSSION

A. METALLOGRAPHY

A typical microstructure of 20-mil sheet is shown in Fig. 4. The etchant was a 1:1 solution of concentrated HCl and HNO<sub>3</sub> with 10 drops of 10% FeCl<sub>2</sub> added per 25 mil of solution.\* There were no appreciable inclusions present among the equiaxed grains with annealing twins (ASTM grain size 8.5). A typical microstructure of 40-mil sheet that consisted of equiaxed grains with annealing twins is shown in Fig. 5. The microstructure did not change with processing. Platelike inclusions were observed with the plate plane parallel to the sheet. These were identified as (Fe, Ni)S. They are assumed to have no effect on longitudinal and transverse properties. The microstructure of rod and tube are shown in Figs. 6 and 7, respectively. The equiaxed grains with annealing twins did not change with processing.

Figure 8 is a scanning electron micrograph of the 40-mil sheet. The two illuminated square areas (A and B) were subjected to energy dispersive analysis of x-rays (EDAX). The results are shown in Figure 9. The y-axis is the intensity and is the total number of x-ray counts accumulated in a given time period. The x-axis is the energy of the x-rays in KeV. The first two peaks correspond to the K<sub>α</sub> and K<sub>β</sub> of Fe, respectively, and the remaining two peaks correspond to the K<sub>α</sub> and K<sub>β</sub> of Ni, respectively. The bars in Fig. 9 correspond to iron and nickel peaks in the grain boundary area, whereas the white dots correspond to a similar scan of the grain interior, as indicated in Fig. 8. There was no relative difference in iron and nickel intensity between the two regions. EDAX of the rod showed similar results. These results indicate that the Ni and Fe are uniformly distributed in the Invar.

B. MECHANICAL PROPERTIES

Mechanical properties included hardness, yield strength (YS), and ultimate tensile strength (UTS), Young's modulus, and percent elongation.

\* T. J. Bertone, The Aerospace Corporation, private communication, June 1976.

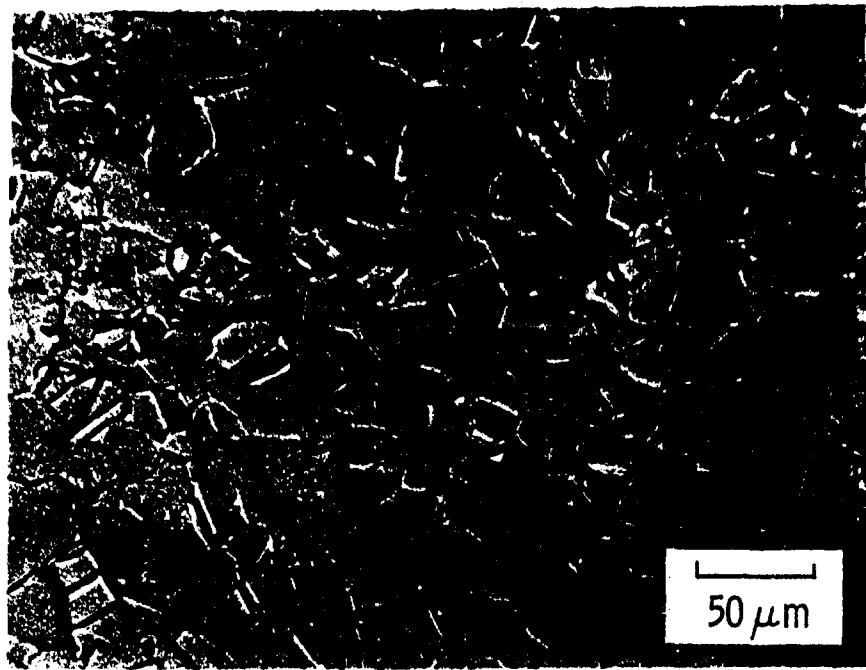


Fig. 4. Optical micrograph of as-received Invar 20-mil sheet in longitudinal direction

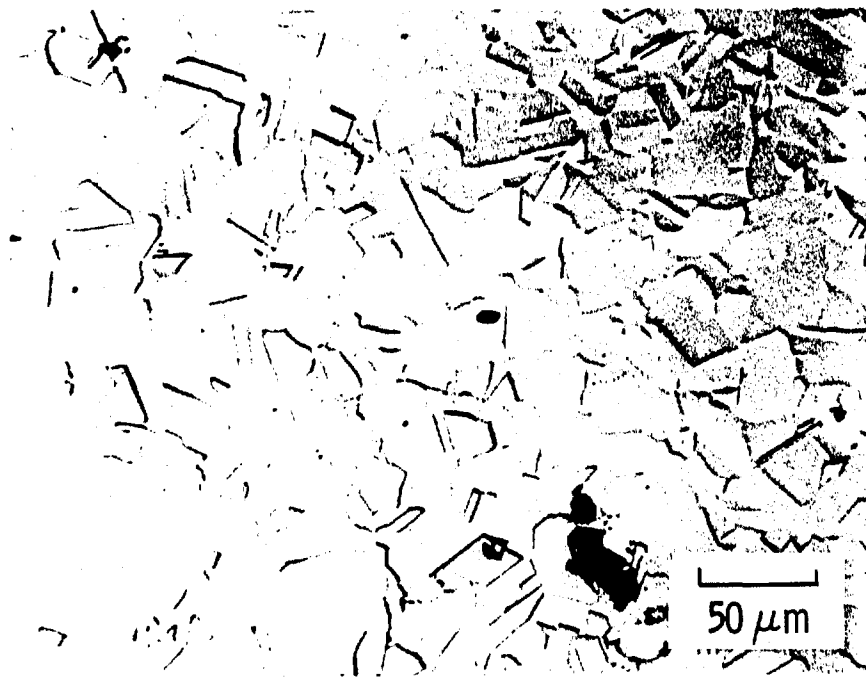


Fig. 5. Optical micrograph of Invar 40-mil sheet (40-2 heat treatment) in longitudinal direction

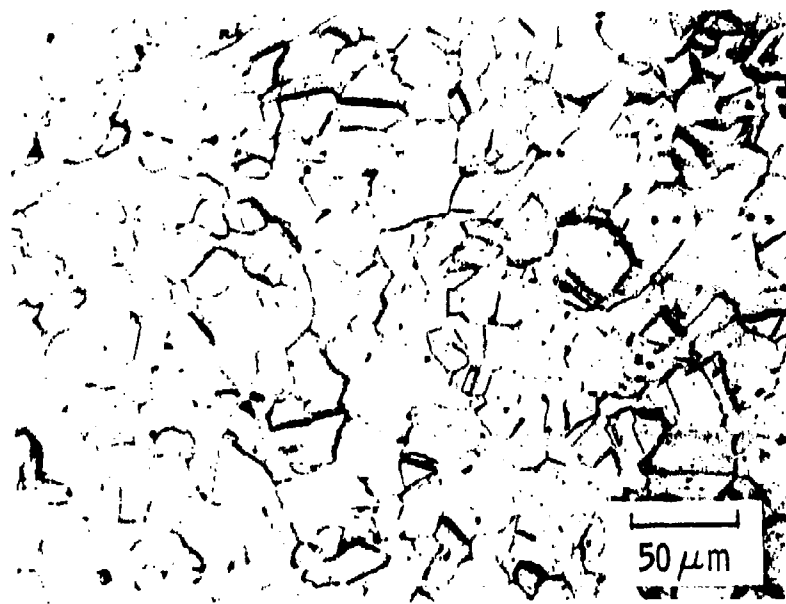


Fig. 6. Optical micrograph of Invar rod (R-1 heat treatment) in radial direction

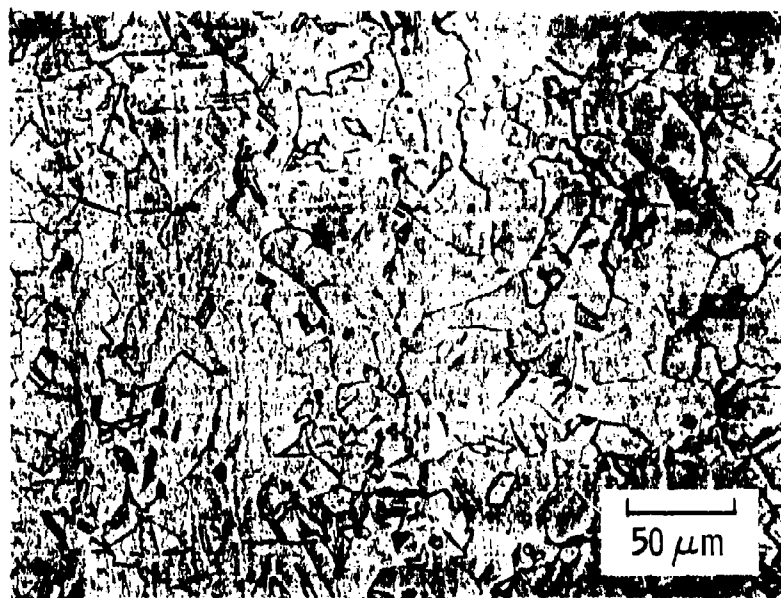


Fig. 7. Optical micrograph of Invar tube (T-1 heat treatment) in radial direction

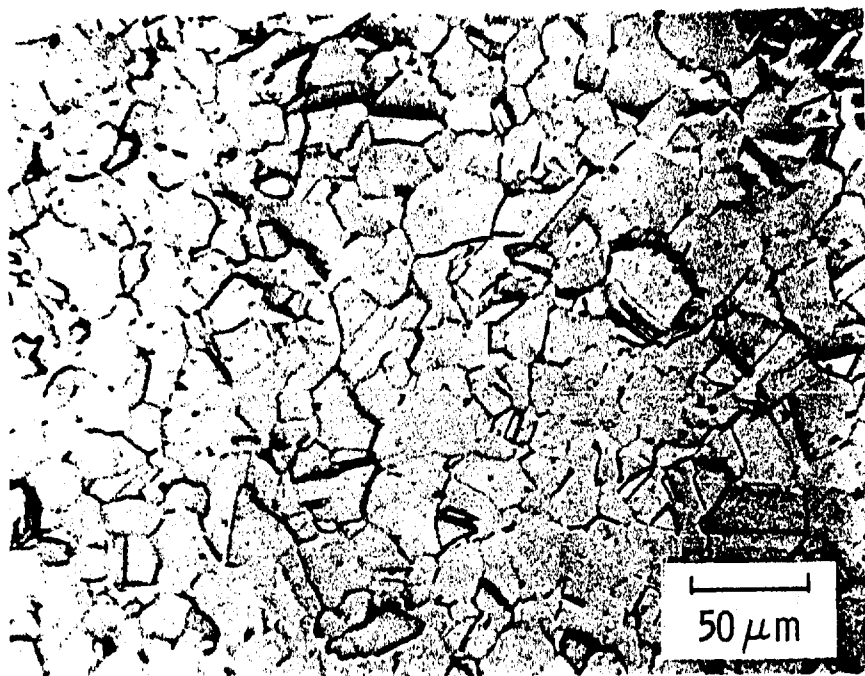


Fig. 6. Optical micrograph of Invar rod (R-1 heat treatment) in radial direction

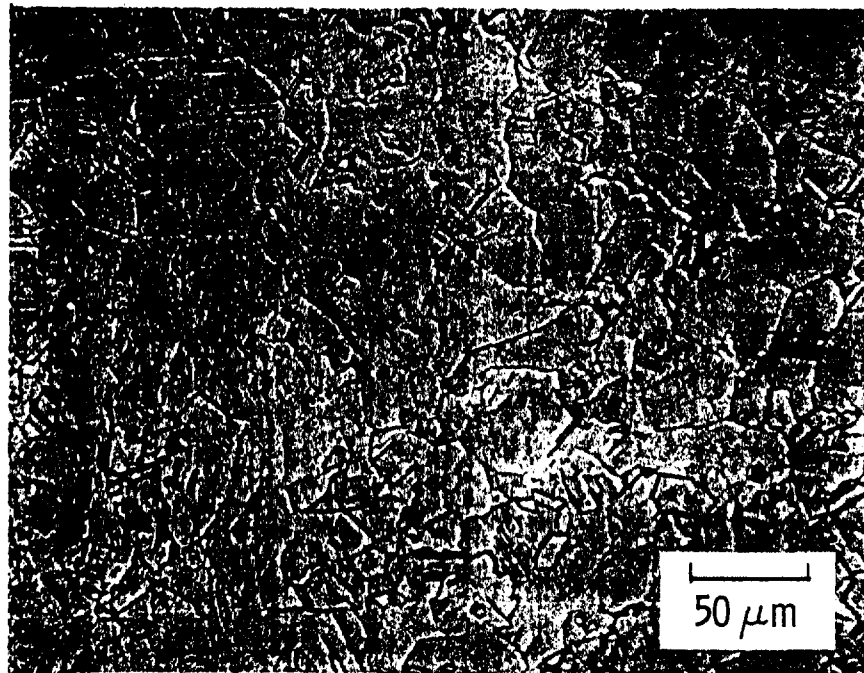


Fig. 7. Optical micrograph of Invar tube (T-1 heat treatment) in radial direction

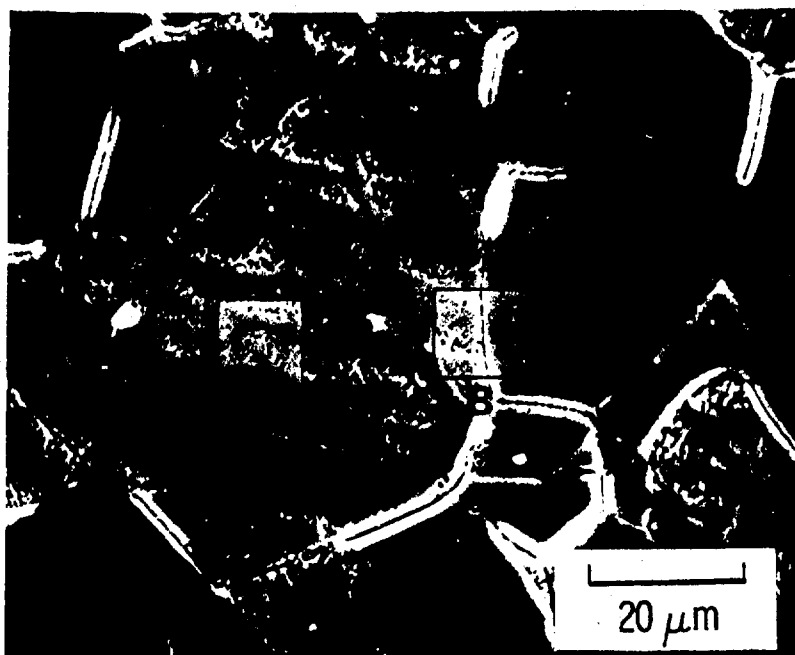


Fig. 8. SEM micrograph of Invar 40-mil sheet (40-1 heat treatment) in longitudinal direction showing square areas A and B used for EDAX

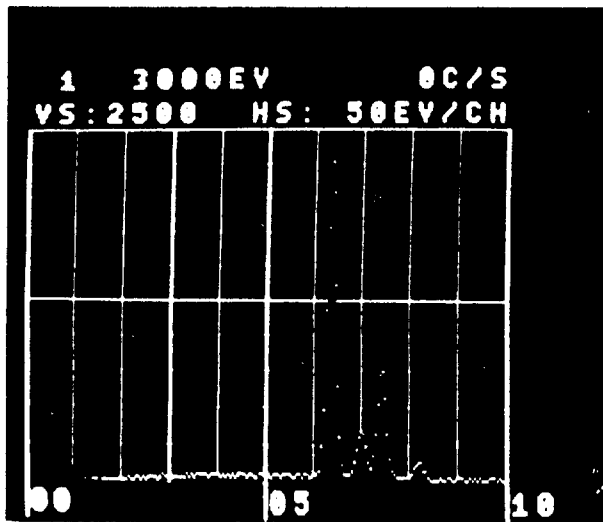


Fig. 9. EDAX of Invar 40-mil sheet in square areas A and B shown in Fig. 8. The two highest intensities correspond to Fe and Ni, respectively

Results are summarized in Table III. Standard deviations given are based on 3 to 6 samples. The YS of the sheet is higher than the YS of the rod. The higher YS is attributed to longitudinal stretching. Increase in longitudinal stretching increased the YS. The YS in the longitudinal direction is higher than in the transverse direction. The thermal treatments, i.e., -1 and -2, given to the AR sheet did not significantly affect the YS. The YS of the rod was not significantly affected by the various thermal treatments. The UTS and elongation of the sheet are not significantly affected by thermal-mechanical processing.

### C. MICROYIELD STRENGTH

The microyield strength results are summarized in Table III. The mean represents 3 - 6 tests. When no standard deviation is given, only one MYS test was performed.

Thermal treatments R-1, R-2, and R-3 represent practical approaches to different combinations of dimensional stability and thermal expansion coefficients. The R-1 heat treatment for the rod is based on the studies of Lement<sup>12</sup> and Eberly<sup>13</sup> to achieve a combination of low thermal expansion with good dimensional stability. The 315°C thermal treatment is effective in relieving the high residual compressive stresses formed at the surface by quenching from 830°C but raises the thermal expansion coefficient. The 96°C thermal treatment essentially completes the  $\gamma$ -expansion with a net expansion of approximately 50  $\mu$ e. The R-2 thermal treatment includes a 205°C thermal treatment that also relieves residual stresses but does not raise the thermal expansion coefficient as high as the R-1. The thermal treatment at 70°C only partially completes the  $\gamma$ -expansion, which causes dimensional instability. The R-3 thermal treatment produces a dimensionally stable structure, but has a high thermal expansion coefficient.<sup>6</sup> The MYS was the same for R-1 and R-2 thermal treatment; R-3 thermal treatment gave the highest MYS. The increase in MYS of the rod is attributed to the slow furnace cool from 830°C. The increase in the MYS of the tube is also attributed to the slow furnace cool from 370°C. However, the nearly twofold increase in

Table III. Microyield Strength and Mechanical Properties of Invar Shapes

Shape and Process	Microyield Strength (ksi)	Yield Strength (ksi)	Ultimate Tensile Strength (ksi)	Young's Modulus (10 <sup>6</sup> ksi)	Elongation (%)
<u>20-mil Sheet</u>					
20-AR L	18.4 ± 1.6	48.6 ± 2.6	72.9 ± 1.6	20.1 ± 1.2	32.5 ± 1.9
20-AR T	18.7 ± 0.6	45.1 ± 1.5	71.9	19.6 ± 1.0	34.0 ± 5.3
20-1 L	18.3 ± 4.8	48.3 ± 4.2	72.7 ± 4.0	18.7 ± 0.1	32.0
20-1 T	19.5 ± 2.8	43.8 ± 3.5	69.5 ± 3.0	19.4 ± 1.5	29.8 ± 1.8
20-2 L	14.8	47.8	72.5	20.8	31
20-2 T	18.8	41.0	68.5	17.8	32
<u>40-mil Sheet</u>					
40-AR		69.9			30
40-1 L	29.7 ± 0.8	50.1 ± 0.3	71.6 ± 0.7	18.8 ± 0.8	33.8 ± 1.6
40-1 T	19.1 ± 0.6	46.1 ± 0.3	70.7 ± 0.4	18.9 ± 0.9	36.2 ± 1.3
40-2 L	28.0 ± 0.6	50.5 ± 1.8	72.4 ± 0.7	19.5 ± 0.5	35.0 ± 2.1
40-2 T	18.4 ± 1.9	47.1 ± 1.2	71.6 ± 0.6	18.9 ± 1.4	34.8 ± 2.8
<u>0.5-in. Rod</u>					
R-1	10.1 ± 0.8	41.4			
R-2	9.9 ± 0.5	40.8			
R-3	13.8 ± 0.4	41.6			
<u>0.5-in. Tube</u>					
T-1		23.6 ± 0.7			

L = longitudinal; T = transverse

the MYS of the tube, which also had a slow cooling step in comparison to the rod, was not resolved. The effect of the R-3 thermal treatment on MYS is consistent with the results of Hemmings and Perkins,<sup>10</sup> who reported that slow cooling in the temperature range 200 to 400°C produces a higher MYS.

The MYS is also increased by stretching. The MYS of 20-mil sheet is increased with 1/2% stretching if 10 ksi is assumed the nominal MYS of annealed Invar.<sup>\*, 7</sup> There is no significant difference between the MYS in the longitudinal and transverse directions. However, the MYS in the longitudinal direction of the 40-mil sheet with 2% stretching is higher than 20-mil sheet, whereas the MYS of 40-mil sheet in the transverse direction is the same as the 20-mil sheet. Although stretching increases the MYS, Ingram et al.<sup>4</sup> reported that plastic prestressing of 2.5 and 5% lowered the MYS of Ni-Span-C. However, the chemical composition and mechanical properties of this material are significantly different from Invar, i. e., chemical composition of Ni-Span-C is typically 0.6% Al, 5.4% Cr, 42.2% Ni, 2.4% Ti, and balance Fe. On the other hand, Marschall<sup>\*</sup> has shown that 35% reduction by cold-working increases the MYS of Invar.

#### D. STRESS VERSUS PLASTIC STRAIN CURVES

Two types of stress-plastic strain behavior are characterized. The 20-mil sheet exhibited a smooth curve as shown in Fig. 10. The 40-mil sheet in the longitudinal direction exhibited an S-shaped curve (Fig. 11), whereas in the transverse direction, the curve was similar to the 20-mil sheet (Fig. 10). The curves for the rod were intermediate.

The curves for the tube material were similar to the 40-mil sheet in the longitudinal direction. Work by several investigators<sup>4, 14, 15</sup> suggests that most materials follow a logarithmic stress-plastic strain relationship of the type

$$\sigma = K \epsilon_p^n$$

<sup>\*</sup>C. W. Marschall, Battelle Columbus Laboratories, private communication, 2 July 1975.

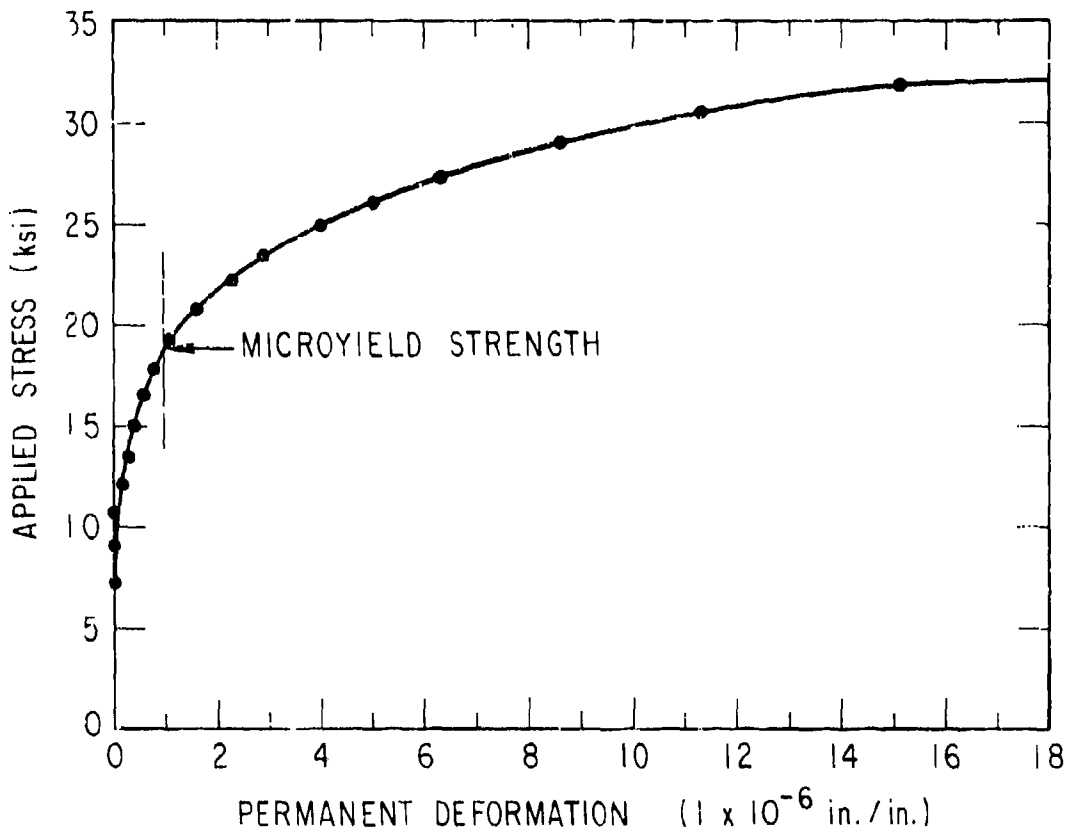


Fig. 10. Stress-plastic strain curve of a 20-mil sheet

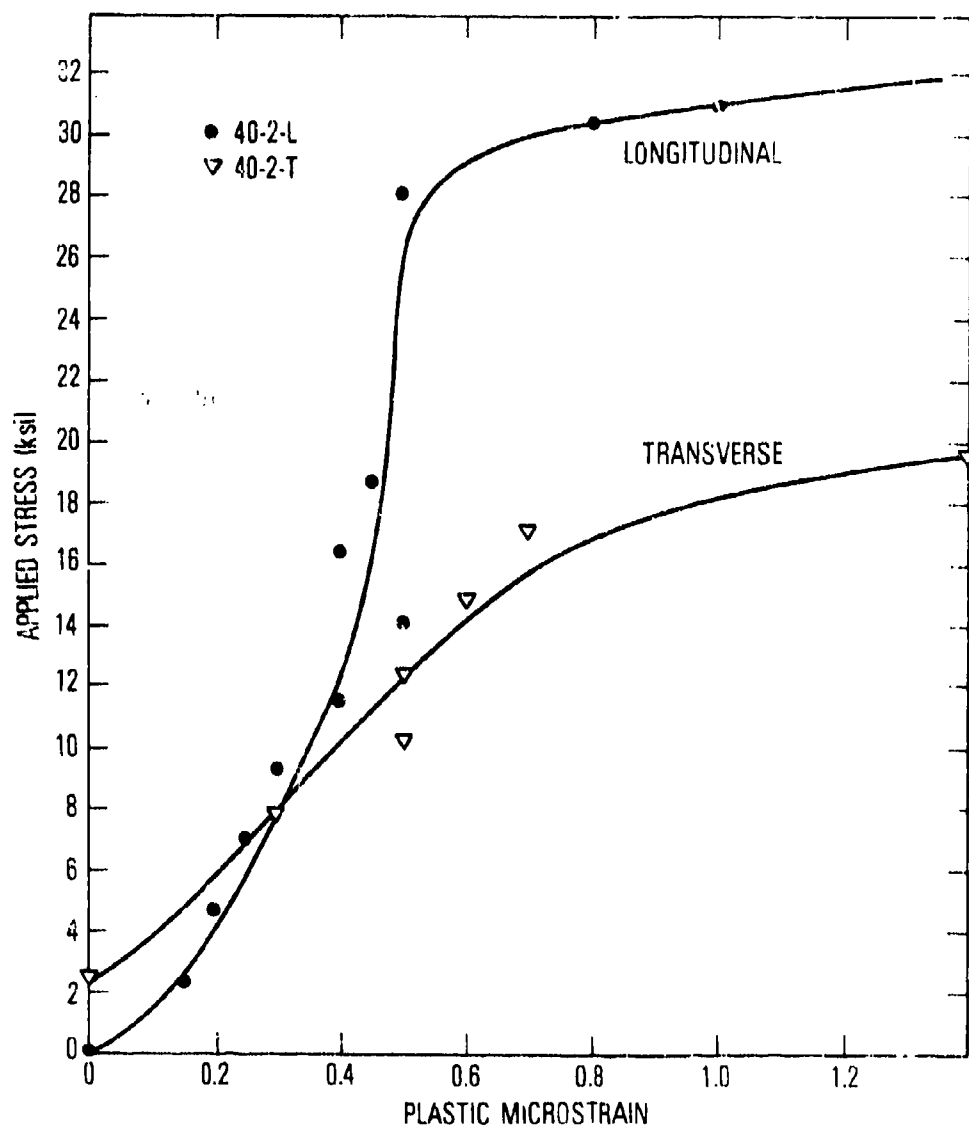


Fig. 11. Stress-plastic strain curves of 40-mil sheet

where  $K$  is the preexponential coefficient,  $n$  is the microstrain hardening exponent, and  $\epsilon_p$  is the plastic strain. A smooth curve (Fig. 10) can be described by one set of  $K$  and  $n$ , whereas an S-shaped curve requires two sets of these parameters (Fig. 12). A statistical analysis of all data was performed. Logarithmic curves were fitted to data below and above the MYS separately and to the combined data. The values of the coefficient of correlation ( $R$ ) and the number of experimental data points ( $N$ ) are given in Table IV. Only in the case of the 40-mil sheet in the longitudinal direction did  $R$  for data below the MYS exceed  $R$  for the combined data. This signified that the data for the 40-mil sheet in the longitudinal direction is more accurately described by two sets of  $K$  and  $n$  rather than one set of  $K$  and  $n$ .

The data described by two sets of  $K$  and  $n$  suggest that other deformation processes are beginning to occur due to the 2% stretching. In comparing the combined data curves, neither  $n$  nor  $K$  showed any significant trend with thermal mechanical processing for any particular shape. The 20-mil sheet has the highest  $K$  values and lowest  $n$  values, whereas the rod has the lowest  $K$  values and highest  $n$  values.

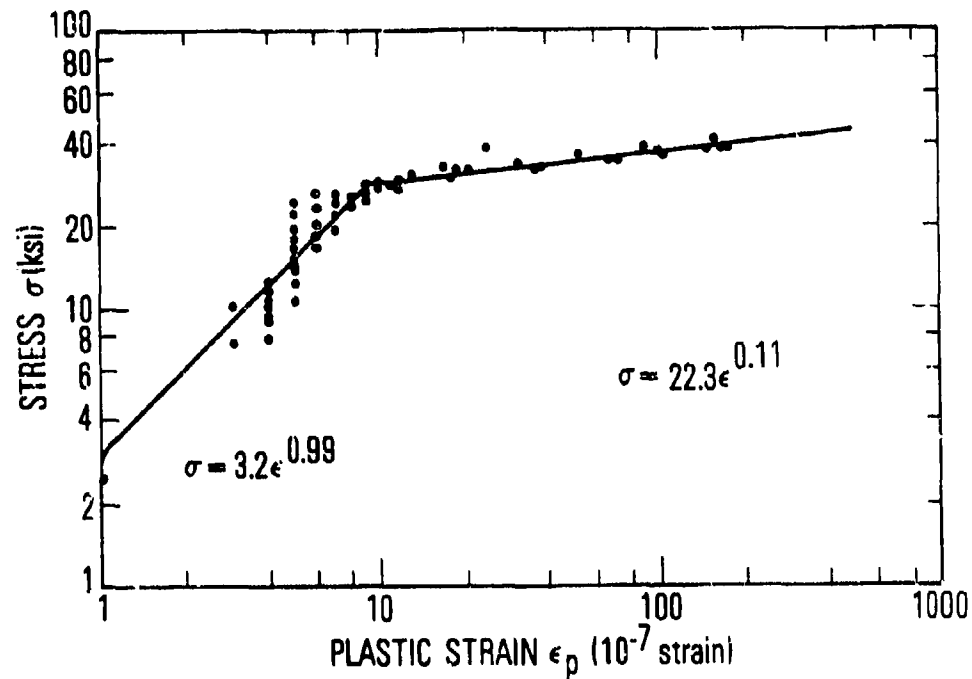


Fig. 12. Log-log plot of stress-plastic strain curve of 40-mil sheet (40-2-L)

Table IV. Results\* from Statistical Analysis for the Determination of K and n

Shape and Process	$10^{-7} \leq \epsilon_p \leq 10^{-6}$			$10^{-6} \leq \epsilon_p \leq 3 \times 10^{-5}$			$10^{-7} \leq \epsilon_p \leq 3 \times 10^{-5}$			
	K	n	R	K	n	R	K	n	R	N
<u>20-mil Sheet</u>										
20-AR-L	10.6	0.21	0.78	24	12.4	0.20	0.91	43	10.6	0.24
20-AR-T	10.1	0.27	0.95	11	15.1	0.12	0.96	14	11.6	0.19
20-1-L	11.8	0.19	0.55	19	11.3	0.20	0.72	21	11.9	0.19
20-1-T	12.8	0.19	0.59	29	15.6	0.10	0.69	27	13.2	0.14
20-2-L	11.8	0.27	0.94	4	14.7	0.28	0.94	12	13.5	0.33
20-2-T	18.9	0.20	0.86	5	17.3	0.23	0.99	4	16.7	0.12
<u>40-mil Sheet</u>										
40-1-L	2.8	1.2	0.79	45	23.4	0.11	0.98	29	10.7	0.32
40-1-T	5.6	0.55	0.76	29	15.3	0.10	0.98	26	9.0	0.24
40-2-L	3.2	0.99	0.87	51	22.3	0.11	0.96	28	7.5	0.28
40-2-T	5.4	0.50	0.58	36	13.9	0.12	0.87	24	9.1	0.35
<u>1/2-in.-diam Rod</u>										
R1	2.0	0.80	0.87	24	6.4	0.22	0.89	28	3.5	0.38
R2	2.7	0.60	0.60	24	6.3	0.19	0.99	27	4.0	0.30
R3	3.5	0.64	0.70	36	8.6	0.23	0.98	28	5.1	0.36
<u>1/2-in.-diam Tube</u>										
T-1	5.2	0.68	0.62	44	18.4	0.10	0.95	24	7.3	0.35
										64

\*  $\epsilon_p$  is in units of  $10^{-7}$  (strain) when calculating  $\sigma$  (ksi).

#### IV. CONCLUSIONS

The microyield strength increases with slow furnace cooling from temperatures  $> 390^{\circ}\text{C}$ .

The microyield strength of sheet in the longitudinal and transverse directions increases with up to 2% longitudinal stretching. Two percent stretching produces a higher microyield strength in the longitudinal direction than in the transverse direction.

Most stress-plastic strain curves can be described with the empirical relationship  $\sigma = K \epsilon_p^n$ . In the case of 40 mil sheet with 2% stretching the stress-plastic strain curves are divided into two segments and are described with two sets of K and n.

## REFERENCES

1. J. S. Marsh, Alloys of Iron and Nickel, Vol. 1, Special Purpose Alloys, McGraw-Hill Book Co., Inc., New York, (1938) pp. 135-183.
2. W. S. McCain, and R. E. Maringer, Mechanical and Physical Properties of Invar and Invar-Type Alloys, DMIC Memorandum No. 207 (31 August 1965).
3. P. F. Weihrauch and M. J. Hordon, The Dimensional Stability on Selected Alloy Systems, AD613931 Alloyd General Corp., Navy Contract N 140(131)-75-98B (August 1964).
4. A. G. Ingram, R. E. Maringer, and F. C. Holden, Study of Microplastic Properties and Dimensional Stability of Materials, AFML-TR-67-232, Wright-Patterson Air Force Base, Columbus, Ohio (August 1968).
5. L. M. Shetky, The Properties of Metals and Alloys of Particular Interest in Precision Instrument Construction, R-137, MIT Instrumentation Laboratory, Cambridge, Massachusetts (January 1957).
6. UNISPAN LR 35 Composition Specifications, Universal Cyclops Specialty Steel Division, Pittsburgh, Pennsylvania
7. G. W. Geil and I. J. Feinberg, Microplasticity I - Measurement of Small Microstrains at Ambient Temperatures, Report No. 9996 (1969) and Microplasticity II - Microstrain Behavior of Normalized 4340 Steel and Annealed Invar, Report No. 9997, National Bureau of Standards, Washington, D. C.
8. G. W. Geil, I. J. Feinberg, and R. B. Clough, "Temperature Changes in Specimens in Microplasticity Tests," Met. Trans. 1, 1845-1851 (1970).
9. P. L. Hemmings and R. A. Perkins, "The Effect of Thermal Treatments in the Micromechanical Behavior of Invar," presented at ASM, Materials Science Seminar, Cincinnati, Ohio, November 1973.
10. C. W. Marschall, "Lowering the Thermal Expansivity of Invar by Decarburization," Proceedings of the 21st National SAMPE Symposium, Los Angeles, 6-8 April 1976, SAMPE, Azusa, California (1972).

11. Strain Gage Installations With Certified M-Bond 200 Adhesives, Instruction Bulletin B-127-2 (July 1971), Micro-Measurements Division of Vishay Intertechnology, Inc., Road, Romulus, Michigan.
12. B. S. Lement, B. L. Averbach, and M. Cohen, "The Dimensional Behavior of Invar," Trans. ASM, 43, 1072-1097 (1951).
13. W. S. Eberly, "How to Make Invar Stay Put," Prod. Eng. 28, 80-81, (1957).
14. C. W. Marshall and R. E. Maringer, "Stress Relaxation as a Source of Dimensional Instability," J. Mater. 6, 374-387, June (1971).
15. R. E. Maringer, M. M. Cho, and F. C. Holden, Stability of Structural Materials for Spacecraft Applications, "Contract No. NAS5-10267, NASA-CR-97844, NASA, Washington, D.C. (16 April 1968).

## LABORATORY OPERATIONS

The Laboratory Operations of The Aerospace Corporation is conducting experimental and theoretical investigations necessary for the evaluation and application of scientific advances to new military concepts and systems. Versatility and flexibility have been developed to a high degree by the laboratory personnel in dealing with the many problems encountered in the nation's rapidly developing space and missile systems. Expertise in the latest scientific developments is vital to the accomplishment of tasks related to these problems. The laboratories that contribute to this research are:

Aerophysics Laboratory: Launch and reentry aerodynamics, heat transfer, reentry physics, chemical kinetics, structural mechanics, flight dynamics, atmospheric pollution, and high-power gas lasers.

Chemistry and Physics Laboratory: Atmospheric reactions and atmospheric optics, chemical reactions in polluted atmospheres, chemical reactions of excited species in rocket plumes, chemical thermodynamics, plasma and laser-induced reactions, laser chemistry, propulsion chemistry, space vacuum and radiation effects on materials, lubrication and surface phenomena, photo-sensitive materials and sensors, high precision laser ranging, and the application of physics and chemistry to problems of law enforcement and biomedicine.

Electronics Research Laboratory: Electromagnetic theory, devices, and propagation phenomena, including plasma electromagnetics; quantum electronics, lasers, and electro-optics; communication sciences, applied electronics, semi-conducting, superconducting, and crystal device physics, optical and acoustical imaging; atmospheric pollution; millimeter wave and far-infrared technology.

Materials Sciences Laboratory: Development of new materials; metal matrix composites and new forms of carbon; test and evaluation of graphite and ceramics in reentry; spacecraft materials and electronic components in nuclear weapons environment; application of fracture mechanics to stress corrosion and fatigue-induced fractures in structural metals.

Space Sciences Laboratory: Atmospheric and ionospheric physics, radiation from the atmosphere, density and composition of the atmosphere, aurorae and airglow; magnetospheric physics, cosmic rays, generation and propagation of plasma waves in the magnetosphere; solar physics, studies of solar magnetic fields; space astronomy, x-ray astronomy; the effects of nuclear explosions, magnetic storms, and solar activity on the earth's atmosphere, ionosphere, and magnetosphere; the effects of optical, electromagnetic, and particulate radiations in space on space systems.

THE AEROSPACE CORPORATION  
El Segundo, California

PRECEDING PAGE, BLANK, NOT FILMED

#### LABORATORY OPERATIONS

The Laboratory Operations of The Aerospace Corporation is conducting experimental and theoretical investigations necessary for the evaluation and application of scientific advances to new military concepts and systems. Versatility and flexibility have been developed to a high degree by the laboratory personnel in dealing with the many problems encountered in the nation's rapidly developing space and missile systems. Expertise in the latest scientific developments is vital to the accomplishment of tasks related to these problems. The laboratories that contribute to this research are:

Aerophysics Laboratory: Launch and reentry aerodynamics, heat transfer, reentry physics, chemical kinetics, structural mechanics, flight dynamics, atmospheric pollution, and high-power gas lasers.

Chemistry and Physics Laboratory: Atmospheric reactions and atmospheric optics, chemical reactions in polluted atmospheres, chemical reactions of excited species in rocket plumes, chemical thermodynamics, plasma and laser-induced reactions, laser chemistry, propulsion chemistry, space vacuum and radiation effects on materials, lubrication and surface phenomena, photo-sensitive materials and sensors, high precision laser ranging, and the application of physics and chemistry to problems of law enforcement and biomedicine.

Electronics Research Laboratory: Electromagnetic theory, devices, and propagation phenomena, including plasma electromagnetics; quantum electronics, lasers, and electro-optics; communication sciences, applied electronics, semi-conducting, superconducting, and crystal device physics, optical and acoustical imaging; atmospheric pollution; millimeter wave and far-infrared technology.

Materials Sciences Laboratory: Development of new materials; metal matrix composites and new forms of carbon; test and evaluation of graphite and ceramics in reentry; spacecraft materials and electronic components in nuclear weapons environment; application of fracture mechanics to stress corrosion and fatigue-induced fractures in structural metals.

Space Sciences Laboratory: Atmospheric and ionospheric physics, radiation from the atmosphere, density and composition of the atmosphere, aurorae and airglow; magnetospheric physics, cosmic rays, generation and propagation of plasma waves in the magnetosphere; solar physics, studies of solar magnetic fields; space astronomy, x-ray astronomy; the effects of nuclear explosions, magnetic storms, and solar activity on the earth's atmosphere, ionosphere, and magnetosphere; the effects of optical, electromagnetic, and particulate radiations in space on space systems.

THE AEROSPACE CORPORATION  
El Segundo, California